

See discussions, stats, and author profiles for this publication at: <https://www.researchgate.net/publication/233972084>

Nanoresolution Radiology of Neurons

Article in *Scientific Reports* · August 2012

DOI: 10.1088/0022-3727/45/24/242001

CITATIONS

16

READS

188

13 authors, including:



Yong S Chu

Brookhaven National Laboratory

268 PUBLICATIONS 4,178 CITATIONS

[SEE PROFILE](#)



Raymond Conley

Argonne National Laboratory

77 PUBLICATIONS 1,450 CITATIONS

[SEE PROFILE](#)



Nathalie Bouet

Brookhaven National Laboratory

53 PUBLICATIONS 631 CITATIONS

[SEE PROFILE](#)

Some of the authors of this publication are also working on these related projects:



Electronic Structure of High Temperature Superconductors [View project](#)



Nano-positioning [View project](#)

Nanoresolution radiology of neurons

This article has been downloaded from IOPscience. Please scroll down to see the full text article.

2012 J. Phys. D: Appl. Phys. 45 242001

(<http://iopscience.iop.org/0022-3727/45/24/242001>)

View [the table of contents for this issue](#), or go to the [journal homepage](#) for more

Download details:

IP Address: 140.109.103.227

The article was downloaded on 30/05/2012 at 07:04

Please note that [terms and conditions apply](#).

FAST TRACK COMMUNICATION

Nanoresolution radiology of neurons

H R Wu^{1,2}, S T Chen¹, Y S Chu³, R Conley³, N Bouet³, C C Chien¹,
H H Chen¹, C H Lin¹, H T Tung¹, Y S Chen¹, G Margaritondo⁴, J H Je⁵
and Y Hwu^{1,2,6,7}

¹ Institute of Physics, Academia Sinica, Taipei, 115, Taiwan

² Department of Engineering and System Science, National Tsing Hua University, Hsinchu 300, Taiwan

³ NSLS-II, Brookhaven National Laboratory, Upton, NY 11973-5000, USA

⁴ Faculté des Sciences de Base, Ecole Polytechnique Fédérale de Lausanne (EPFL), CH-1015 Lausanne, Switzerland

⁵ X-ray Imaging Center, Department of Materials Science and Engineering, Pohang University of Science and Technology, Pohang 790-784, Korea

⁶ Advanced Optoelectronic Technology Center, National Cheng Kung University, Tainan 701, Taiwan

E-mail: phhwu@sinica.edu.tw

Received 10 April 2012, in final form 3 May 2012

Published 29 May 2012

Online at stacks.iop.org/JPhysD/45/242001

Abstract

We report recent advances in hard-x-ray optics—including record spatial resolution—and in staining techniques that enable synchrotron microradiology to produce neurobiology images of quality comparable to electron and visible microscopy. In addition, microradiology offers excellent penetration and effective three-dimensional detection as required for many neuron studies. Our tests include tomographic reconstruction based on projection image sets.

(Some figures may appear in colour only in the online journal)

Recent directions in neurobiology increasingly require advanced imaging with subcellular resolution and three-dimensional view [1]. Microradiology has made rather impressive advances and could become a good candidate for this task. Are its performances adequate, however? Our results show that they are mainly because of two factors: a new record in spatial resolution and *ad hoc* staining optimized for x-rays—rather than developed for other microscopies.

The best evidence for this conclusion is provided by the images themselves. Figure 1 shows a typical example: a patchwork microradiograph of neurons from mouse cerebellum, sectioned to 50 μm and stained as discussed later. The bottom part shows a magnified portion of the picture. The estimated Rayleigh contrast lateral resolution (see below) is better than 20 nm. The contrast and the overall image quality are comparable to the best visible and electron micrographs.

In addition, images like that of figure 1 bring important features not delivered by optical or electron microscopy. First, the penetration of hard-x-rays (8 keV here) is much larger

than that of electrons or visible photons. As in common radiology, this facilitates the internal analysis of systems—in this case, the interior of cells or the inner structure of complex neuron networks. Second, high penetration allows tomographic reconstruction and three-dimensional rendition. This is quite important, for example, when analysing the intricate features of neuron networks.

What makes results like figure 1 possible now, in contrast to previous years? The first factor is resolution. We obtained record levels with our imaging procedure, described in detail in [2]—which exploits x-rays emitted by the 32-ID [3] beamline of the advanced photon source (APS), Argonne National Laboratory, and by the BL 01B [4, 5] beamline of the National Synchrotron Radiation Research Center (NSRRC), Hsinchu, Taiwan. The core of the microscopy systems is a Fresnel zone plate magnifying lens, which determines the imaging resolution. Specifically, the spatial resolution of the zone plate is defined by the width of the outermost zone and by the diffraction order [6, 7].

The recent progress by different groups in diffractive optics for x-rays was quite impressive [8–12]. In particular,

⁷ Author to whom any correspondence should be addressed.

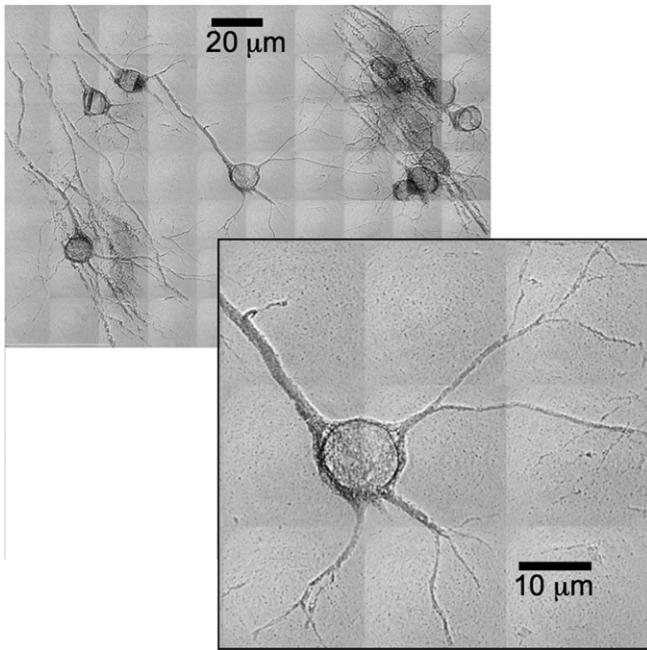


Figure 1. An example of high-resolution microradiology image of neurons, and a magnified portion (bottom).

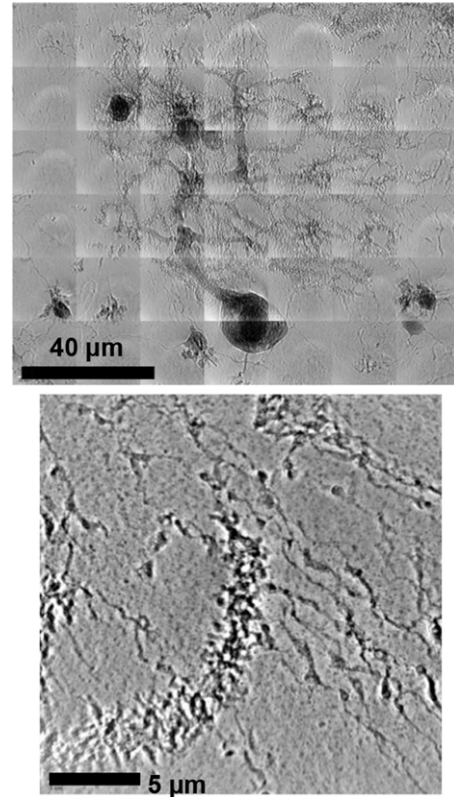


Figure 3. Top: microradiograph of neurons (including a Purkinje cell in the lower part). Bottom: magnified portion revealing the neuron dendritic spine.

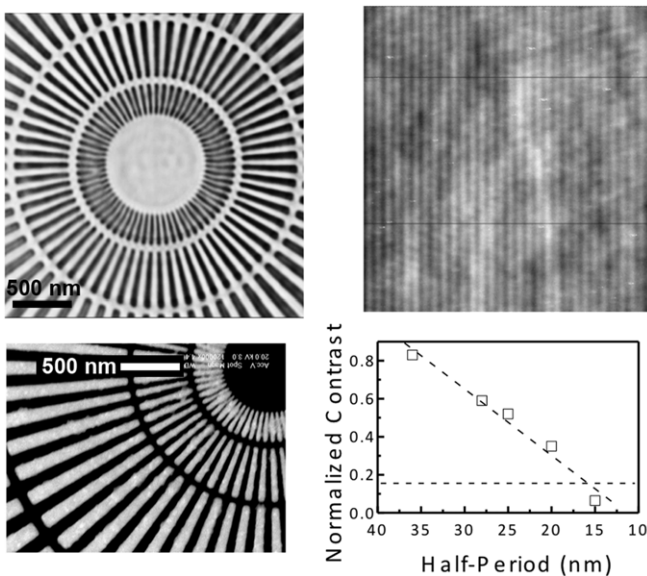


Figure 2. Experimental tests demonstrating a Rayleigh contrast spatial resolution well below 20 nm. The scale bar on the bottom-left also applies to the top-left image.

we obtained zone plates with a nanostructure suitable for hard-x-rays [13–17] and an outermost zone of 20 nm. Figure 2 shows an example of resolution evaluation. On the top-left part, we see the image of a test pattern with visible features down to 20 nm. The bottom-left picture is a scanning electron microscope (SEM) image demonstrating that the previous micrograph matches its capability to reveal the smallest features.

The top-right part is a micrograph of another test pattern, a periodic multilayer of Si and WSi₂ with 15 nm layer width—again, clearly visible. For a quantitative resolution assessment, we fabricated several multilayers such as that of the top-right

image with different widths of the Si and WSi₂ layers. From the corresponding images, we derived the Michelson contrast, $(I_{\max} - I_{\min}) / (I_{\max} + I_{\min})$, where I_{\max} and I_{\min} are the minimum and maximum intensities in line scans along the multilayer structure (we used for reference the absorption of wide Si and SiW₂ regions on the sides of each multilayer). The contrast is plotted on the bottom-right part of figure 2 as a function of the layer thickness.

The dashed horizontal line corresponds to the Rayleigh contrast resolution criterion. The interpolation demonstrates a Rayleigh contrast resolution of ≈ 16.5 nm—to the best of our knowledge, the most advanced for hard-x-rays. We repeated the resolution tests with different zone plates, different test patterns and also using power spectrum analysis [18]. The results consistently indicated resolution levels below 20 nm.

To avoid misunderstandings, we note that the notion of ‘Rayleigh contrast resolution’ is linked, but not equivalent, to that of ‘Rayleigh resolution’ which deals with diffraction effects: two points are resolved if their separation is larger than the distance between one point and the first minimum of its diffraction-caused Airy pattern. The corresponding minimum intensity I_{\min} (at the midpoint) is $\approx 73.5\%$ of the peak intensity I_{\max} of each point. In terms of contrast, $(I_{\max} - I_{\min}) / (I_{\max} + I_{\min}) \approx (1 - 0.735) / (1 + 0.735) \approx 15.3\%$, the value of figure 2. We also note that even with contrast well below the Rayleigh criterion features can still be visible if the noise is sufficiently low; this is the case, for example, of the top-right image in figure 2.

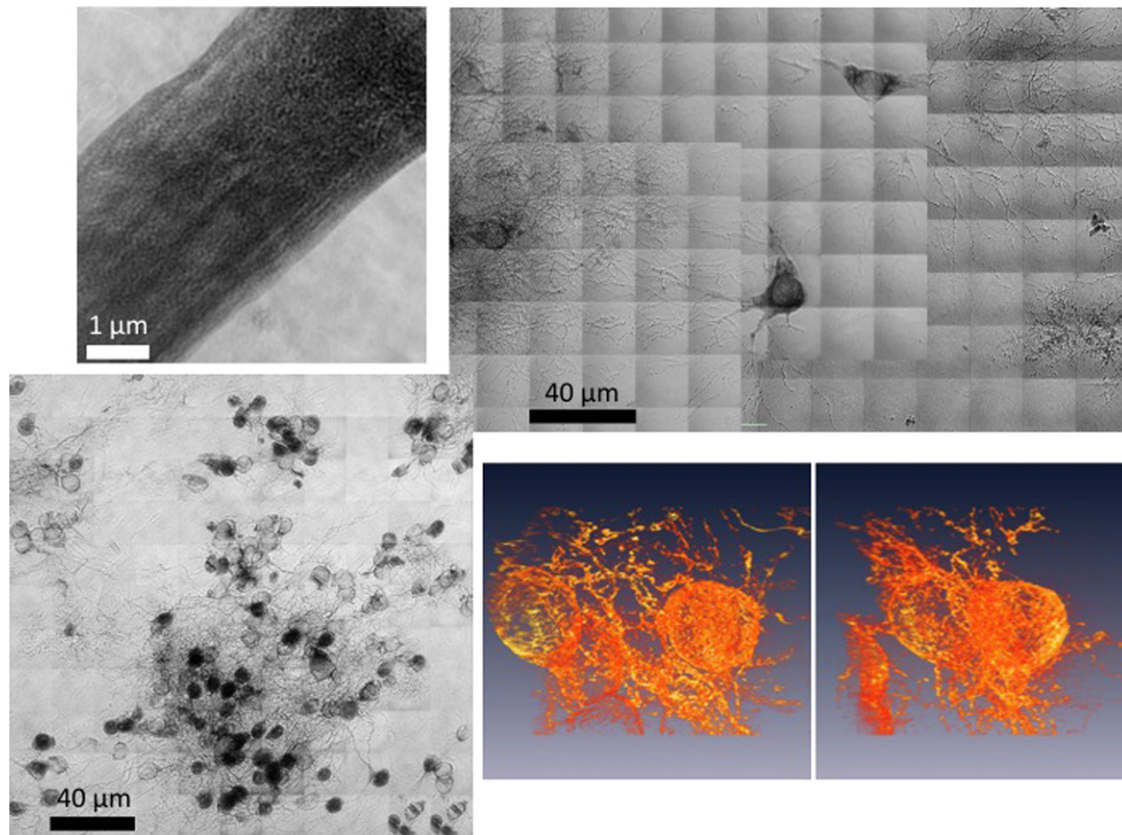


Figure 4. Top-left: image of an axon coated with staining ingredient particles. Top-right: broadview image including multipolar neurons. Bottom-left: image of a dense neuron cluster demonstrating the capability to reveal cells in the deep layers. Bottom-right: two three-dimensional reconstructed images from a microtomography test (field of view: $20\ \mu\text{m}$).

The second factor making possible results like figure 1 is staining. Staining procedures are crucial in neurobiologic microscopy [19, 20]. Unfortunately, the effective technical solutions developed for optical microscopy cannot be transferred to microradiology.

The main problem is the perfusion of the staining ingredient: in optical microscopy, the penetration of fluorophores is adequate for the thin specimens, typically tens of micrometres. But this is not sufficient for x-rays, whose specimens reach hundreds of micrometres. Furthermore, the fluorescent ingredients cannot really enhance x-ray contrast, which requires instead heavy elements [21].

We performed a long search for a suitable staining procedure before finding the solution in a modified Golgi-Cox approach [22]. In the standard Golgi-Cox method, mercury and silver can produce sufficient high x-ray contrast. Without changing the ingredients, we extended the incubation time to one month or more. This augmented the perfusion and produced staining over the entire depth of our microradiology specimens.

The Academia Sinica Institutional Animal Care and Utilization Committee (AS IACUC) approved all procedures involving animals. The brain specimens were from 5–8 weeks old BALB/c ByJNarl mice from the National Laboratory Animal Center (NLAC) in Taiwan; we washed them with 0.4M Sorenson's phosphate buffer (PBS), then put them for at least 30 days in Golgi-Cox solution in the dark at room

temperature. Afterwards, we transferred them for 2–3 days in 30% sucrose solution in PBS for cryoprotection. We then performed coronal sectioning with a Thermo Fisher Scientific Shandon Cryotome obtaining $200\ \mu\text{m}$ slices. The sections were treated as described by Gibb and Kolb [23], dehydrated and embedded in epoxy resin on plastic coverslips.

We obtained x-ray micrographs with 8 keV photons filtered by a double-crystal monochromator, with a typical measurement rate of 0.5 s per frame. For tomography reconstruction we used sets of 280 projections spaced by 0.5° . For additional details on the imaging procedure, see [24].

Figures 3 and 4 show further evidence of the high quality of our neuroimages and illustrate several additional features. Note for example in figure 3, bottom, the magnified part of the top image: we can see the details of the neuron dendritic spine [25]. This demonstrates that we can detect fine details at the subcellular level.

The top-left image of figure 4 shows an axon coated with particles of the staining ingredient. The size of such particles is 30–50 nm and the corresponding spatial resolution, once again, exceeds 20 nm.

The top-right part of the figure illustrates how three-dimensional imaging leads to the morphology-based identification of different neurons and neuron parts: we see, in particular, multipolar neurons [26]. Also note the Purkinje (astrocyte) [27] morphology of the largest neuron in figure 3.

The bottom-left image of figure 4 stresses the importance of staining and penetration while imaging complex networks.

Individual neurons are indeed clearly visible not only in the first layer but also below. Finally, the two bottom-right images are three-dimensional tomography reconstructions of two neurons from two different points of view (from 280 projection images at 0.5° intervals, details in [28]). Thus, our approach can be implemented in the tomographic mode, enhancing the three-dimensional analysis.

Further technical improvements are certainly possible: efforts are specifically underway to refine the staining procedure and increase the percentage of stained cells [29]. We are also further refining the zone plate fabrication method. However, even without such additional progress microradiology is already capable of detecting and analysing fine details—and contributing to neurobiology research.

Acknowledgments

The authors thank T Y Chen and Y T Chen for preparing the zone plates. The research is supported by the National Science and Technology for Nanoscience and Nanotechnology, the Academia Sinica, the Fonds National Suisse pour la Recherche Scientifique, the EPFL, the Center for Biomedical Imaging (CIBM), and the Brookhaven Science Associates, LLC under Contract No DE-AC02-98CH10886. Use of the advanced photon source is supported by the US Department of Energy, Office of Basic Energy Sciences, under Contract No DE-AC02-06CH11357.

References

- [1] Kim J *et al* 2011 *Sci. Rep.* **1** 122
- [2] Chen T Y, Chen Y T, Wang C L, Kempson I M, Lee W K, Chu Y S, Hwu Y and Margaritondo G 2011 *Opt. Express* **19** 19919
- [3] Shen Q, Lee W K, Fezzaa K, Chu Y S, De Carlo F, Jemian P, Ilavsky J, Erdmann M and Long G G 2007 *Nucl. Instrum. Methods A* **582** 77
- [4] Yin G C, Song Y F, Tang M T, Chen F R, Liang K S, Duewer F W, Feser M, Yun W and Shieh H-P D 2006 *Appl. Phys. Lett.* **89** 221122
- [5] Song Y F *et al* 2007 *J. Synchrotron Radiat.* **14** 320
- [6] Attwood D 1999 *Soft X-Rays and Extreme Ultraviolet Radiation: Principles and Applications* (Cambridge: Cambridge University Press)
- [7] Yi J, Chu Y S, Chen Y-T, Chen T-Y, Hwu Y and Margaritondo G 2011 *J. Phys. D: Appl. Phys.* **44** 232001
- [8] Vila-Comamala J, Gorelick S, Färm E, Kewish C M, Diaz Ana, Barret R, Guzenko V A, Ritala M and David C 2011 *Opt. Express* **19** 175, and the references therein
- [9] Vila-Comamala J *et al* 2010 *AIP Conf. Proc.* **1221** 80
- [10] Kaulich B, Thibault P, Gianocelli A and Kiskinova M 2011 *J. Phys. C: Solid State Phys.* **23** 083002, and the references therein
- [11] Mayer M, Grévent C, Szeghalmi A, Knez M, Weigand M, Rehbein S, Schneider G, Baretzky B and Schütz G 2011 *Ultramicroscopy* **111** 1076, and the references therein
- [12] Feng Y, Feser M, Lyon A, Rishton S, Zeng X, Chen S, Sassolini S and Yun W 2007 *J. Vac. Sci. Technol. B* **25** 2004
- [13] Chao W, Harteneck B D, Liddle J A, Anderson E H and Attwood D T 2005 *Nature* **435** 1210
- [14] Chao W, Kim J, Rekawa S, Fischer P and Anderson E H 2009 *Opt. Express* **17** 17669
- [15] Chen Y T *et al* 2008 *Nanotechnology* **19** 395302
- [16] Chen Y T, Chen T Y, Yi J, Chu Y S, Lee W K, Wang C L, Kempson I M, Hwu Y, Gajdosik V and Margaritondo G 2011 *Opt. Lett.* **36** 1269
- [17] Lo T N *et al* 2007 *J. Phys. D: Appl. Phys.* **40** 3172
- [18] Vogt S, Schneider G, Steuernagel A, Lucchesi J, Schulze E, Rudolph D and Schmahl G 2000 *J. Struct. Biol.* **132** 123
- [19] Chen C C, Wu J K, Lin H W, Pai T P, Fu T F, Wu C L, Tully T and Chiang A S 2012 *Science* **335** 678
- [20] Chiang A S *et al* 2010 *Curr. Biol.* **21** 1
- [21] Chien C C *et al* 2012 *Biotechnol. Adv.* at press
- [22] Glaser E M and Van der Loos H 1981 *J. Neurosci. Methods* **4** 117
- [23] Gibb R and Kolb B 1998 *J. Neurosci. Methods* **79** 1
- [24] Chien C-C *et al* 2012 *Biotechnol. Adv.* at press
- [25] Hering H and Sheng M 2001 *Nature Rev. Neurosci.* **2** 881
- [26] Stensaas L J 1967 *J. Comp. Neurol.* **129** 71
- [27] Crepel F, Mariani J and Delhaye-Bouchaud N 1976 *J. Neurobiol.* **7** 567
- [28] Chien C-C, Chen H H, Lai S F, Wu K-C, Cai X, Hwu Y, Petibois C, Chu Y S and Margaritondo G 2012 *J. Nanobiotechnol.* **10** 10
- [29] Li A, Gong H, Zhang B, Wang Q, Yan C, Wu J, Liu Q, Zeng A and Luo Q 2010 *Sci.* **330** 1404